Effect of Au addition on hydrogen permeation and the resistance to H2S on Pd-Ag alloy membranes

Please check the document version of this publication:

• A submitted manuscript is the version of the article upon submission and before peer-review. There can be important differences between the submitted version and the official published version of record. People interested in the research are advised to contact the author for the final version of the publication, or visit the DOI to the publisher's website.
• The final author version and the galley proof are versions of the publication after peer review.
• The final published version features the final layout of the paper including the volume, issue and page numbers.

Link to publication

Effect of Au addition on hydrogen permeation and the resistance to H$_2$S on Pd-Ag alloy membranes

Jon Melendez[a,b], Niek de Nooijer[c], Kai Coenen[c], Ekain Fernandez[a], Jose Luis Viviente[a], Martin van Sint Annaland[c], P.L. Arias[b], D.A. Pacheco Tanaka[a], Fausto Gallucci[c]

[a] TECNALIA. Energy and Environment Division. Mikeletegi Pasealekua 2, 20009 San Sebastián-Donostia, Spain

[b] Chemical Engineering and Environmental Department, University of the Basque Country UPV/EHU,

C/ Alameda Urquijo s/n, 48013 Bilbao, Spain

[c] Chemical Process Intensification, Department of Chemical Engineering and Chemistry, Eindhoven University of Technology, De Rondom 70 5612 AZ Eindhoven, The Netherlands

Abstract

In order to make a detailed comparison between Pd-Ag and Pd-Ag-Au membranes according to their H$_2$ permeation properties and sulfide resistance Au was deposited by the electroless plating (ELP) technique onto one half of Pd-Ag membranes. Permeation tests have been carried out from 400 to 600 °C under single gas conditions. The Pd$_{91.7}$Ag$_{4.8}$Au$_{3.5}$ membrane has shown a H$_2$ permeance of 4.71·10^{-3} mol s^{-1} m^{-2} Pa$^{0.5}$ at 600 °C, which is one of the highest values ever reported in the literature, where the Pd-Ag-Au membranes have exhibited higher hydrogen permeation rates compared to their respective Pd-Ag membranes above 550 ºC. The correlation between the H$_2$ flux and the partial pressure differences between the retentate and permeate sides at different values of n, showed the effect of Au addition on the adsorption dissociation steps. The H$_2$ permeation properties have been determined in terms of the degree of H$_2$S inhibition, up to 17 ppm, and subsequent H$_2$ flux recovery rate. Pd-Ag membranes alloyed with gold resisted 12.5 hours of H$_2$S exposure showing recovery rates of 85 and 83% for Pd$_{91.5}$Ag$_{4.7}$Au$_{3.8}$ and Pd$_{90.5}$Ag$_{4.6}$Au$_{4.9}$ membranes, respectively, whereas the hydrogen flux of non-gold membranes decreased below detectable values. No evidence of the formation of a crystalline sulfide phase on the Pd-Ag-Au alloy membrane surfaces was found in the XRD patterns after H$_2$S exposure and also XPS characterization did not show important changes in the composition before and after the H$_2$S exposure tests. However, SEM images showed a decrease in the thickness of the Pd-Ag membrane and signs of corrosion and roughening on its surface, while gold-alloyed membranes did not show any damage.

Keywords: Palladium-silver-gold membrane; electroless plating; H_2 permeation; H_2S poisoning; H_2 recovery.

Corresponding author
Jon Meléndez, email: jon.melendez@tecnalia.com
Fausto Gallucci, email: f.gallucci@tue.nl

1. Introduction

In the last century, hydrogen has mainly been used as a chemical product and intermediate for different industrial applications (ammonia synthesis, methanol production, petroleum refining, etc.). However, the importance of high purity hydrogen has recently increased due to new and different applications such as micro/nano-electronics, fuel cells, transport and small stationary energy conversion devices (combined heat and power production), chemical and metallurgical industries, as well as in large stationary power installations [1]. Almost 50% of the global production of hydrogen is currently generated via steam methane reforming of natural gas [2]. Hydrogen selective membranes have frequently been used in separation steps or in reactors with the aim of obtaining high feedstock conversion and production of pure H_2. Among those membranes, Pd based membranes have high H_2 permeation and very high perm-selectivity due to their solution/diffusion mechanism, where hydrogen is adsorbed on the surface and dissociated into hydrogen atoms which permeate through the membrane bulk. However, the presence of H_2S impurities can irreversibly poison the Pd membranes. Sulfur is a very common impurity in fossil fuels, especially in coal, biogas and also in natural gas (depending on its origin). The adsorption of H_2S molecules compete with hydrogen for active sites, and increases the energy barrier for hydrogen dissociative adsorption, resulting in a significant decrease in the hydrogen adsorption rate and thus the hydrogen permeance [3]. In particular H_2S can react with the Pd surface to form a Pd_4S phase depending on the exposure conditions, which is not as permeable as pure Pd and is also susceptible to mechanical failure [4] [5] [6]. In fact, the a large difference between the constant lattices of pure Pd and Pd_4S causes structural stresses and leads to the formation of cracks or even the fracture of Pd membranes.

In order to improve stability, Pd membranes are generally alloyed with other metals. The addition of Ag or Cu to Pd can improve the resistance to hydrogen embrittlement below 298 °C and at H_2 pressures above 2MPa. Pd-Ag alloy membranes show higher H_2 permeation rates than pure Pd; when the amount of Ag increases, at 23 wt. %Ag ($Pd_{77}Ag_{23}$), the permeation rate increases up to 1.7 times higher than the H_2 permeation of pure Pd [7]. However, Pd-Ag alloys, as well as pure Pd, are prone to forming bulk sulfides in the presence of H_2S throughout a wide range of exposure conditions [8] [9].

Considerable effort has also been spent on Pd–Cu membranes in order to improve their flux properties, since they do not show embrittlement even at low temperatures [10] [11]. The Pd–Cu

alloy presents some advantages over pure Pd. It gives a maximum hydrogen permeability at approximately $Pd_{60}Cu_{40}$ and, although this does not show higher hydrogen permeability when compared to Pd–Ag alloys, it is mechanically more stable and exhibits resistance to H_2S poisoning [12]. The response of Pd-Cu alloys exposed to H_2S is a complex function of the alloy composition and the exposure conditions [13]. Pd-Cu alloys can form two different crystal structures: body-centered cubic (bcc) and face-centered cubic (fcc), depending on composition and temperature. In this regard, many different proportions of Cu (20-47 wt%) in Pd-alloys were evaluated by Morreale et al. [14] at temperatures ranging from 330 to 750 °C in the presence of 1100 ppm H_2S. A change in the crystal structure of the alloy due to the rearrangement of the Pd and Cu atoms can affect the permeability of the membrane [15].

Although many studies have been performed on Pd-Cu alloy membranes because of their sulfur resistance, Pd–Au alloy composite membranes have received increasing interest mainly due to two reasons: the presence of gold reduces the embrittlement problem resulting from the hydride phase transition and improves the resistance to poisoning and corrosive degradation by sulfur compounds. It has also been reported that the addition of Au also increases the hydrogen permeability compared to pure Pd [16]. Several authors have reported the performance of Pd-Au alloy membranes tested in gas mixtures of H_2S in H_2 streams. Gade et al. [17] observed a 29% H_2 flux inhibition at 500 °C for a $PdAu_{23}$ membrane in a sour WGS mixture containing 20 ppm H_2S. Chen et al. [6] reported resistance to bulk sulfidation of a $PdAu_8$ alloy composite membrane under exposure of 54.8 ppm H_2S/H_2 mixture in the temperature range of 350–500 °C, also proving that the higher permeance recovery occurs at higher temperatures due to the exothermic nature of the dissociative adsorption of H_2S on metals.

Ternary Pd alloys have also been considered more extensively in the recent years for their potential to improve both the permeability and H_2S response. Some researchers as Peters et al. [18], prepared a $Pd_{75}Ag_{22}Au_3$ membrane by magnetron sputtering improving the performance over $Pd_{85}Au_{15}$ and $Pd_{70}Cu_{30}$ membranes in the presence of H_2S. Lewis et al. [19] reported a $PdAu_{20}Ag_{13}$ membrane with a higher hydrogen permeability than a $PdAu_{23}$ alloy in single gas conditions at 400 and 500 ºC and reduction of 52-75% under 20 ppm H_2S conditions between 500 and 400 ºC, pointing out the importance of the temperature on the H_2 flux inhibition. Furthermore, Braun et al. [13], [20] have proved the effectiveness of the addition of gold to high permeability PdAg binary membranes as inhibitor of the sulfur poisoning effect.

The purpose of this work is to investigate the effect of the addition of Au on the H_2 permeation properties of Pd-Ag-Au alloy membranes as a function temperature and the influence of the Au concentration as a function of the H_2S content in the feed gas stream. Starting from Pd-Ag alloy membranes prepared by the electroless plating deposition technique (ELP), only one half of these membranes was used to deposit Au onto it, whereas the binary alloy membrane was kept to be tested at exactly the same conditions as the ternary alloy membranes. Both half membranes (the Pd-Ag alloy and the Pd-Ag-Au one) were placed together in the same reactor module to perform single gas tests which allowed to quantify their permeation properties and their response to different temperatures at the same time and under the same conditions of pressure and gas flow rates leading to a fairer comparison between these membranes. Different gold contents have been evaluated and a detailed characterization of the membranes before and after H_2S exposure has been carried out.

2. Experimental

2.1 Membrane preparation

Thin Pd-Ag layers were deposited on activated asymmetric ceramic tubes using the simultaneous deposition technique previously reported by Tanaka et al. [21], [22] and [23]. The Pd-Ag membranes were annealed at 550 °C for 4 h (3°C/min heating rate), using a 10% H_2 / 90% N_2 gas mixture.

Afterword, two of the Pd-Ag prepared membranes were half covered with teflon tape and a subsequent Au deposition process was carried out onto the uncovered parts for 5 hours; following the process conditions suggested by Okazaki et al. [24] while improving the chemical composition of the plating solution. The concentration of $K[Au(CN)_4]$ was tuned to obtain different % Au compositions. Then, the resulting membranes were composed by a Pd-Ag alloy and a Pd-Ag-Au one (Figure 1).

Five membranes were prepared in total (Table 1). M1 - M1Au having the same Pd-Ag base layer, were tested in the range of 400-600 ºC under single gas conditions and placed together in the same reactor, therefore, the permeation conditions were the same. On the other hand, the influence of H_2S in feed gas stream was studied for M2, M2Au (these two had the same Pd-Ag content) and M3Au membranes.

To determine the composition, from each membrane a sample was taken before any kind of permeation test was performed. The samples were dissolved at 130 °C for 12 h in aqua regia using a Parr´s acid digestion vessel. Then a small amount of this solution was taken and diluted 20 times with deionized water and measured by ICP-OES (Inductively Coupled Plasma - Optical Emission Spectrometry) using a Varian Vista MPX.

Figure 1. Picture of two membranes (half Pd-Ag and half Pd-Ag-Au) prepared by ELP (picture taken before annealing treatment).

2.2 Annealing treatment study

Pd-Ag-Au ternary samples of the M1Au membrane were annealed at 550 °C with different dwell times to monitor the alloy formation. Membrane samples were heated from room temperature to 550 °C at 3 °C/min in nitrogen. Then, the temperature was maintained for 8, 12, 16 and 24 hours. During the dwell time, the flow was changed to a 10% H_2 / 90% N_2 gas mixture with a total flow rate of 500 mL min^{-1}. The cooling step was again carried out only in nitrogen atmosphere. X-ray diffraction experiments were carried out to follow the formation of the alloy.

2.3 Membrane sealing

For the permeation tests, the membranes were cut and sealed using Swagelok® connectors and graphite ferrules, following the procedure reported before in [22], [23] and [25].

2.4 Permeation tests

Single gas permeation experiments were carried out using a reactor of 102 mm in diameter and 1000 mm in height and placed in a three zone oven used to keep the reactor at the desired temperature. The pressure throughout all the tests was measured at the top and the bottom of the reactor. The reactor was designed to have the possibility to test five membranes at the same time and under the same conditions. A complete description of the reactor module is provided in [23].

The influence of H_2S on the H_2 permeance of Pd-Ag and Pd-Ag-Au membranes was studied in an in-house designed setup suitable for membrane tests with H_2S (Figure 2). The membranes were sealed and placed in a reactor. A three zone oven was used to heat up the reactor to the desired operating temperature and was controlled with three independent thermocouples. An additional thermocouple was placed in the inside of the membrane and another thermocouple at the gas outlet of the oven. A gas feeding system with Bronkhorst mass flow controllers was used to produce the desired gas mixtures. 100 ppm of H_2S in H_2 were supplied (Linde HIQ) and mixed with H_2 to get the desired composition of H_2S in the feed gas stream. The pressure in the reactor was controlled by a Bronkhorst back pressure regulator. In addition, the pressure was controlled prior to the reactor in the feed gas line and in the permeate stream. The H_2 permeance was continuously monitored and logged using a Bronkhorst Mini Cori flow meter (up to 2 l/min). The setup is fully automated and controlled by a computer, enabling continuous operation and data acquisition. The N_2 leakage of the membranes was determined with a Horibastec liquid film flow meter.
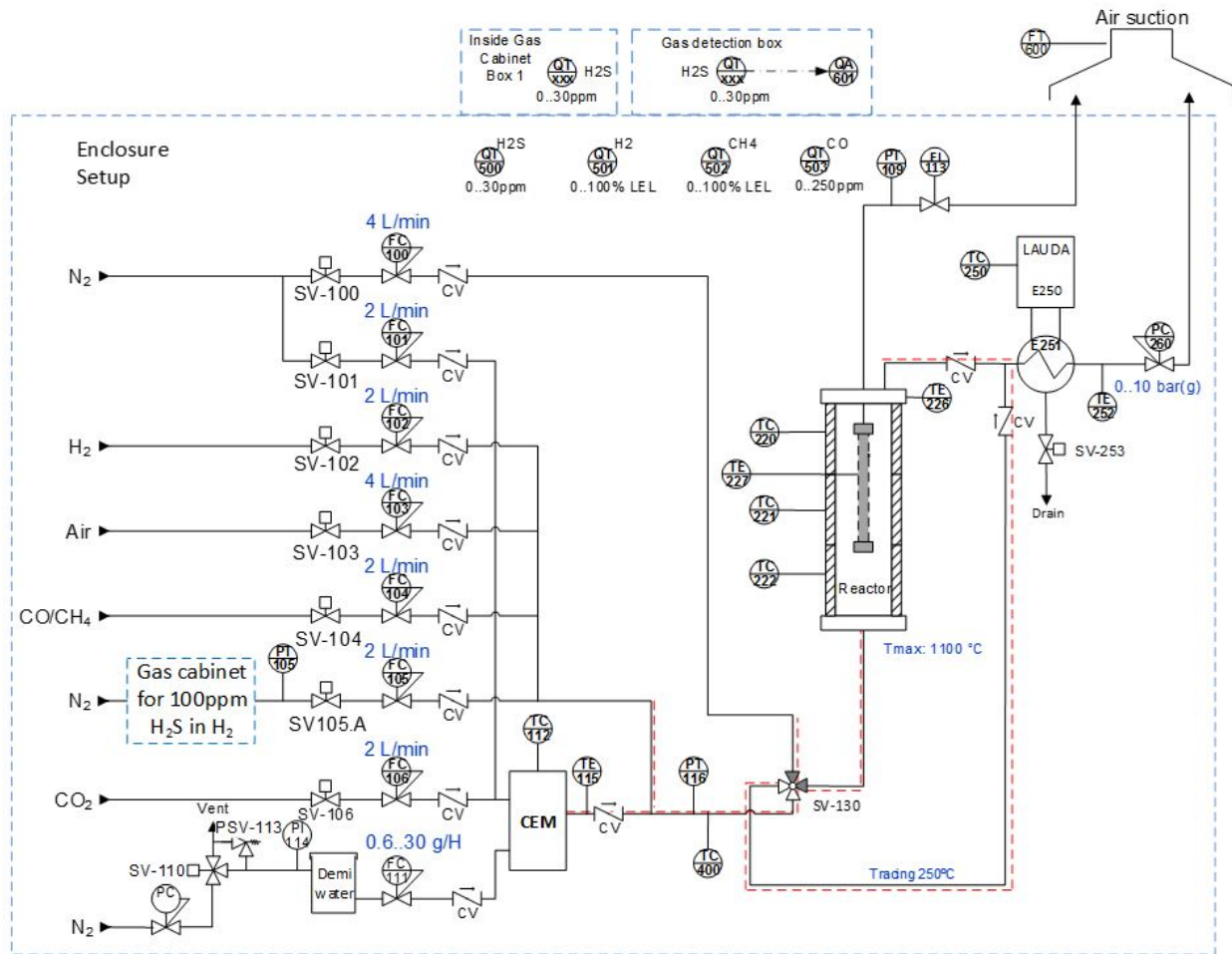
Figure 2. Scheme of the in-house designed setup suitable for tests with H_2S.

2.5 Characterization

A FEI Quanta 250 FEG (Environmental Scanning Electron Microscope; ESEM) equipment was used to determine the thickness and morphology of the membranes. Pd-alloy membranes were characterized by X-ray electronspectometry (XPS) with a monochromatic Thermo Scientific K-Alpha. Spectra were obtained using an aluminium anode (Al Kα = 1486.6 eV) operating at 72 W and a spot size of 400 µm and Sputtering was done with a beam energy of 1000 eV at low current. A MiniFlex 600 Benchtop XRD (X-Ray Diffractometer) was used both to follow the Pd-Ag-Au alloy formation at 550 °C and after permeation tests to detect the presence of any bulk sulfides that may have formed during testing. The scan speed was 1.00 º/min and the step width 0.02°, in the range 2θ = 30-90º with a Kβ radiation at 40 kV and 15 mA.

3. Results and discussion

3.1 Physico-chemical and structure characterization

The studied membranes and their compositions, determined by ICP-OES, are listed in Table 1.

Table 1. ICP analysis of membranes prepared in this study.

Membrane / Code	%Pd	%Ag	%Au
Membrane 1 (Pd-Ag) / M1	94.9	5.1	-
Membrane 1 (Pd-Ag-Au) / M1Au	91.7	4.8	3.5
Membrane 2 (Pd-Ag) / M2	96,1	3,9	-
Membrane 2 (Pd-Ag-Au) / M2Au	91,5	4,7	3,8
Membrane 3 (Pd-Ag-Au) / M3Au	90,5	4,6	4,9

Once the deposition of Au by ELP over a Pd-Ag alloyed membrane was carried out, the membranes were exposed to a thermal treatment under nitrogen flow during the heating step at 550 ºC and subsequently in a mixture of hydrogen and nitrogen (10/90 %vol.). Different dwell times at 550 ºC (8, 12, 16 and 24 hours) were used to study the formation of a ternary alloy using XRD post-characterization. In Figure 3a the XRD spectra of $Pd_{91.7}Ag_{4.8}Au_{3.5}$ (membrane M1Au) are shown in a range of $2\Theta = 30º - 90º$ after Au deposition at 550 ºC and various annealing times. Figure 3b displays the same XRD diffraction patterns as Figure 3a, but for $2\Theta = 35º - 45º$ to show the evolution of the main peak of the alloy as a function of time in greater detail.

The red line shows the XRD diffraction of the $Pd_{94.9}Ag_{5.1}$ (M1) membrane after 4 hours of annealing at 550 °C and after gold deposition, but without thermal treatment. With this characterization the evolution of diffracted peaks can be monitored from the beginning. The spectra (red line) shows Pd-Ag alloyed peaks at 2Θ diffracted from the planes (1 1 1), (2 0 0), (2 2 0), (3 1 1) and (2 2 2) respectively and, four new peaks corresponding to Au are observed. After every annealing test, the membrane exhibits only the peaks for the $Pd_{91.7}Ag_{4.8}Au_{3.5}$ (M1Au) alloy without the presence of the Pd-Ag and Au as separated peaks. During annealing, the Au peaks shifted to higher diffraction angles. The asymmetrical shapes of the Pd-Ag-Au alloy peaks

after 8 and 12 hours of thermal treatment (blue and green lines, respectively), indicate that ternary alloying is not complete yet; especially in the higher planes like (1 1 1) and (2 0 0) in the region of Pd-Ag. After 16 and 24 hours of annealing (yellow and black lines respectively), the main peak (1 1 1) of the Pd-Ag alloy is shifted to a lower 2Θ showing similar behavior as reported by Gade et al. [26] for annealing treatments above 400 ºC and also by Peters et al. [18] when comparing the Pd-Ag-Au ternary alloy with the Pd-Ag layer. This symmetry of the (1 1 1) diffracted peak after 16 and 24 hours of thermal treatment can be better observed in Figure 3b. The calculated lattice parameter of the Pd-Ag-Au main peak was 3.924 Å.
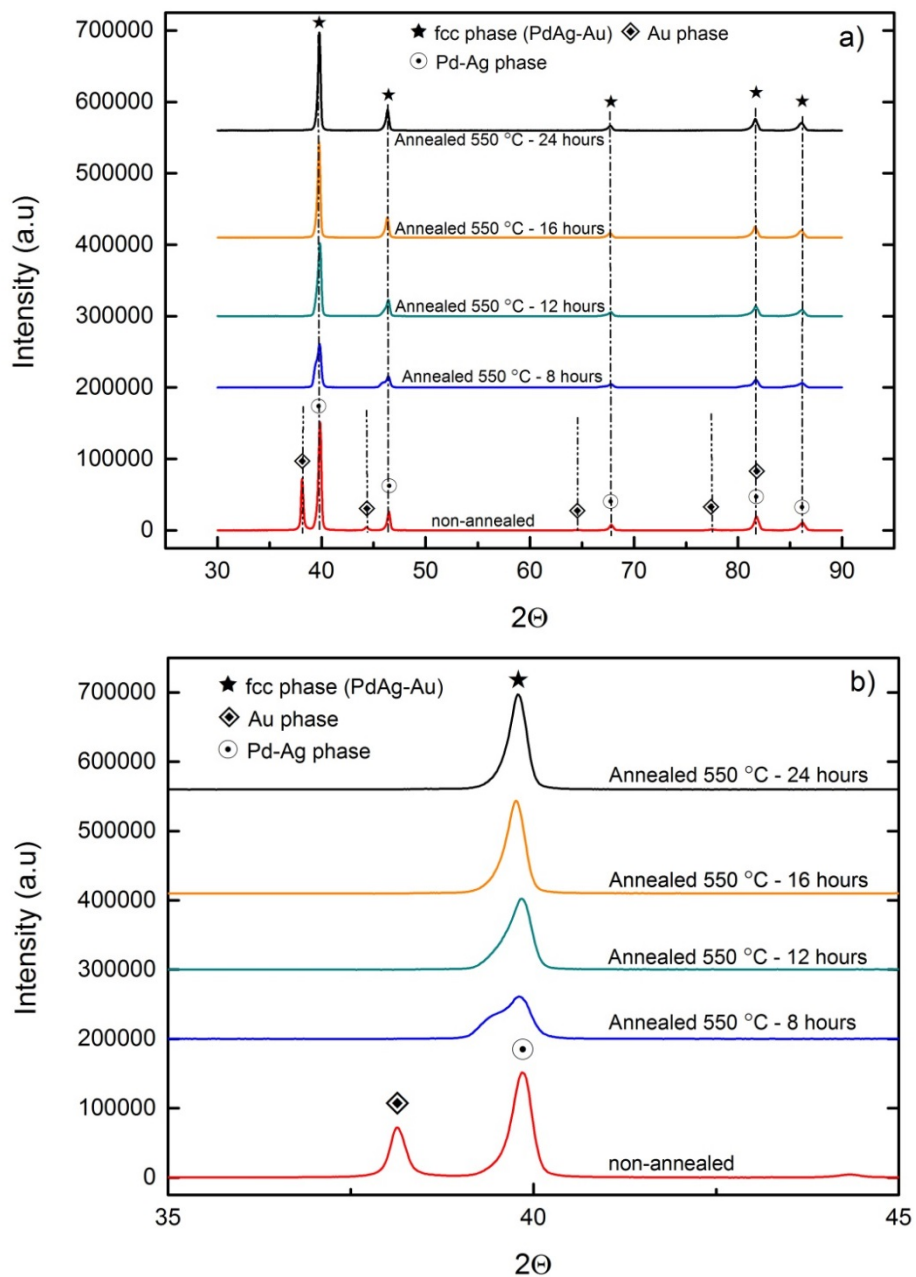
Figure 3. XRD spectra at a) $2\Theta = 30° - 90°$ and b) $2\Theta = 35° - 45°$ of $Pd_{91.7}Ag_{4.8}Au_{3.5}$ (M1Au) after Au deposition (represented with a red line) and after a subsequent annealing process at 550 °C during 8 hours (blue line), 12 hours (green line), 16 hours (orange line) and 24 hours (black line).

SEM characterization of the cross-section of all the membranes before and after the addition of gold was performed in order to calculate their thicknesses (figures not reported here). Membranes M1 and M1Au, which will be used in single gas conditions to test the hydrogen

permeation at different temperatures showed 2.95 ± 0.25 μm and 2.71 ± 0.19 μm (thicknesses without and with Au, respectively. The M2, M2Au and M3Au membranes, which will be further tested under H_2S atmosphere with different concentrations, had a thickness of 2.53 ± 0.25, 3.13 ± 0.09 and 2.42 ± 0.15 μm, respectively. Only a small increase in the thickness was found after Au addition to M2, but when considering the standard deviation of the cross-section measurements with SEM, the differences can be considered negligible.

3.2 Permeation and characterization results of thin Pd-Ag and Pd-Ag-Au supported membranes

3.2.1 Single gas permeation test

The hydrogen and nitrogen fluxes through $Pd_{94.9}Ag_{5.1}$ (M1) and $Pd_{91.7}Ag_{4.8}Au_{3.5}$ (M1Au) membranes were evaluated together in the multi-membrane reactor described in [23] at various pressures (ranging from 1 to 3 bar of total pressure) and temperatures (between 400 and 600 °C) in order to study the effect of Au addition onto the M1 membrane on the permeation properties. In the reactor, both membranes were tested at exactly the same conditions of temperature, pressure difference and time obtaining thus comparable results. The setup was heated up to 400 °C and the membranes were activated following the activation protocol in order to remove organic impurities on the membrane surface as reported in [23]. The H_2 flux of the activated membranes was measured at different temperatures and pressure differences across the membrane.

In order to determine the value of *n*, a fit through the H_2 flux data to pressure differences was evaluated for different values of *n* and the linear regression factor r^2 was determined and this is shown in Figure 4. The highest value of r^2 is not obtained with *n* = 0.5 for $Pd_{91.7}Ag_{4.8}Au_{3.5}$ (M1Au) (Figure 4b), showing that the permeation characteristics of the composite membrane follows a slightly different permeation mechanism than the Sieverts–Fick [7]. This behavior has also been found by Iulianelli et al. [27] for a $PdAu_7$ dense layer supported on a porous stainless steel (PSS) support at 420 °C. However, $Pd_{94.9}Ag_{5.1}$ (M1) as depicted in Figure 4a, showed its highest regression factor with *n* = 0.5 in the range 400-500 °C and with *n* = 0.6 at 550 °C and 600 °C, confirming that the addition of Au leads to an increasing importance of adsorption dissociation as rate limiting step instead of bulk transport in the solution-diffusion model for hydrogen permeation. Figure 5 shows the H_2 permeation flux as a function of the the difference

of the squareroot of the pressure between the retentate and permeate sides in the range 400-600 °C for the $Pd_{91.7}Ag_{4.8}Au_{3.5}$ (M1Au) membrane.
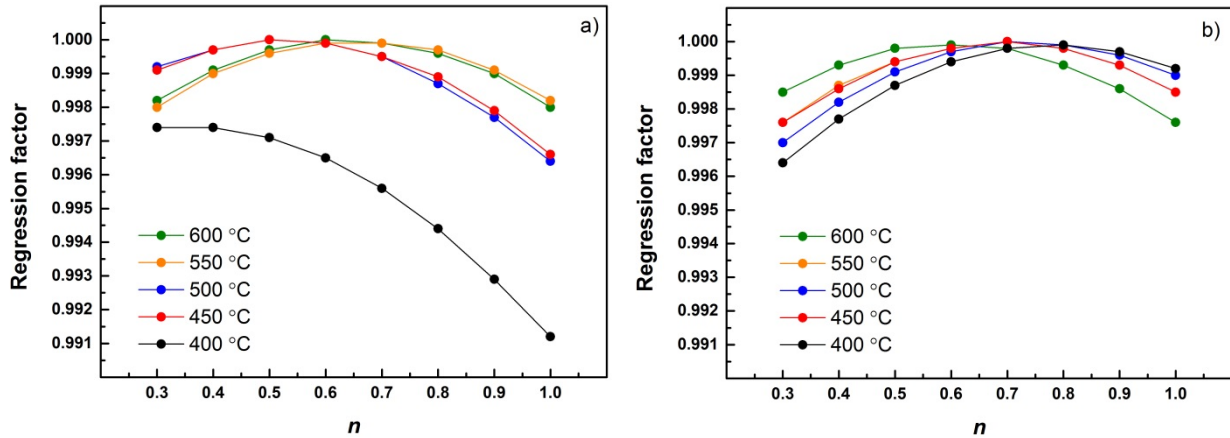

Figure 4. Regression factor of H_2 flux versus different transmembrane pressures with various values of *n* for a) M1 and b) M1Au in a range of temperatures from 400 °C to 600 °C.
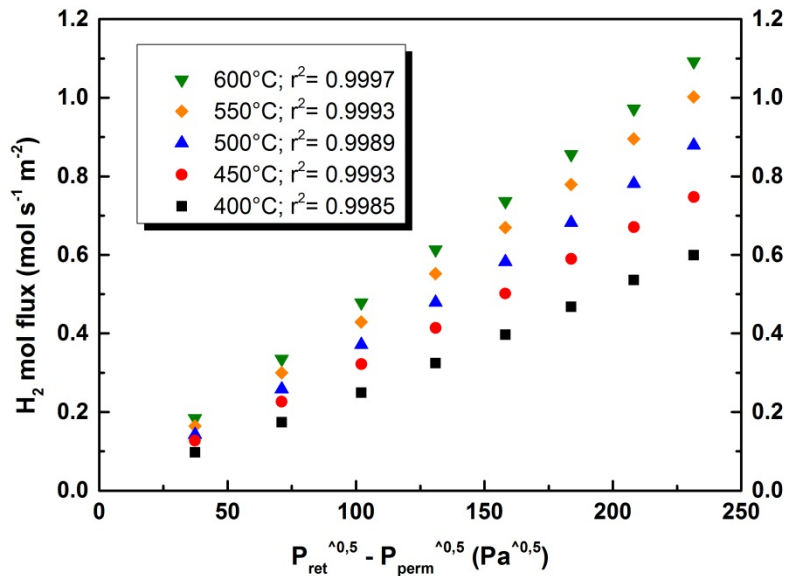

Figure 5. Hydrogen flux through the $Pd_{91.7}Ag_{4.8}Au_{3.5}$ (M1Au) membrane as a function of difference of square root of the hydrogen pressure on the retentate and permeate sides at different temperatures

From the permeation studies at different temperatures, the activation energies of H_2 permeation of the M1 and M1Au membranes were calculated using the Arrhenius equation as shown in Figure 6. For M1 ($Pd_{94.9}Ag_{5.1}$) an Ea of 9.5 kJ mol^{-1} was obtained, which is within the range of

similar Pd-Ag alloy membranes reported by our group [28] (10 kJ mol^{-1} for a 4µm thick $Pd_{85}Ag_{15}$ membrane). On the other hand, the Ea for $Pd_{91.7}Ag_{4.8}Au_{3.5}$ membrane was 16.0 kJ mol^{-1} which is exactly the same as found by Braun et al. for a $PdAu_{22}Ag_8$ membrane [13]. Since in this work the permeation experiments were carried out in the same reactor at the same conditions and the base PdAg membrane is the same, the previous results suggest that the addition of small amounts of Au influences the permeation mainly in the adsorption dissociation step, which is favored by the presence of Au on the surface as demonstrated in Figure 4.
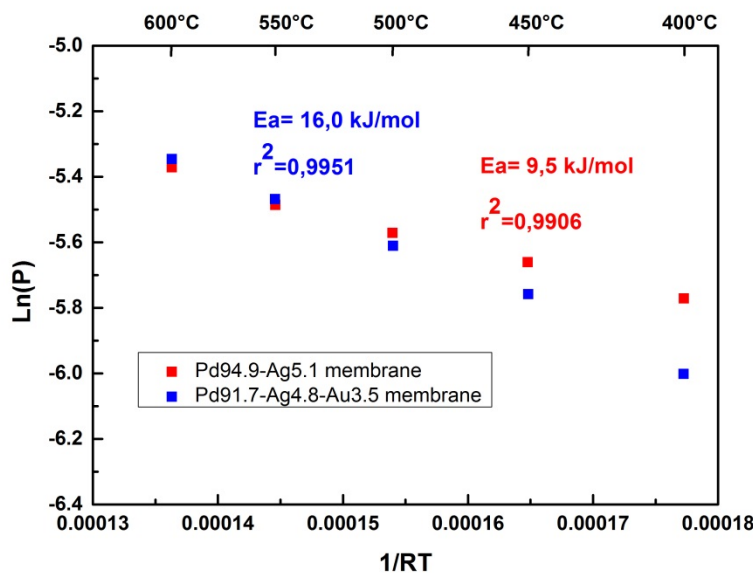

Figure 6. Determination of the activation energy (*Ea* in kJ mol^{-1}) of H2 permeation of the M1 ($Pd_{94.9}Ag_{5.1}$) and M1Au ($Pd_{91.7}Ag_{4.8}Au_{3.5}$) membranes

The differences in H_2 permeation between the membranes M1 and M1Au are depicted in Figure 7, which shows the H_2 flux at 100 kPa pressure difference from 400 °C to 600 °C. It can be observed that at temperatures lower that 500 °C the H_2 permeation of M1 is higher than M1Au. However, at 550 °C or higher, M1Au overtakes M1 in terms of hydrogen flux. This could be explained by the ability of Au to dissociate H_2 at high temperatures.
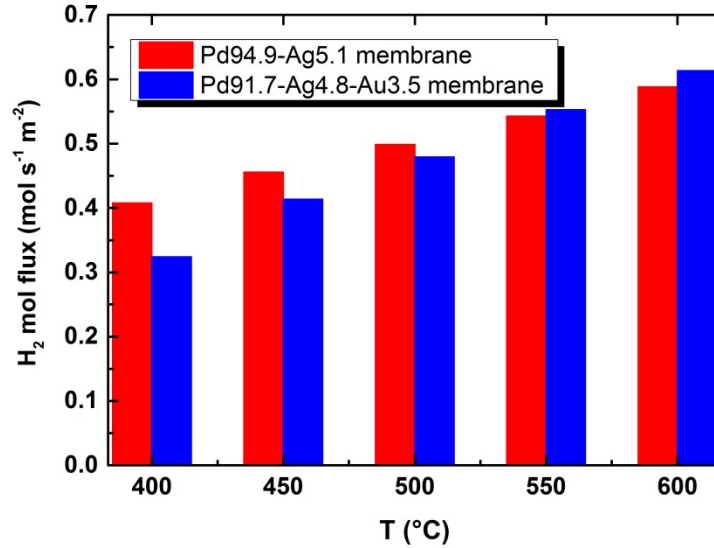
Figure 7. Comparison of hydrogen flux of $Pd_{94.9}Ag_{5.1}$ (M1) and $Pd_{91.7}Ag_{4.8}Au_{3.5}$ (M1Au) at 100 kPa pressure difference from 400 °C to 600 °C.

Only a few studies were found in the literature that correlate the hydrogen permeability, temperature and Au composition for Pd-Au membranes. These include the works reported by McKinley [8] at 350 °C, both theoretical calculations for 350 °C and 500 °C by Catalano et al. [29] and Gryaznov research [30] at 500 °C. The ratio between the hydrogen flux of Pd-Au and Pd membranes increases until around 10 wt% Au at 350 °C and 500 °C. After this point, the H_2 flux slowly decreases down to zero when the Au % overcomes 50 %.

The M1 ($Pd_{94.9}Ag_{5.1}$) and M1Au ($Pd_{91.7}Ag_{4.8}Au_{3.5}$) membranes were tested for 150 h at 600 °C and 1 bar pressure difference in order to assess its long-term performance. The H_2 and N_2 flow rates were monitored over time to determine the evolution of the H_2 permeance and the H_2/N_2 ideal perm-selectivity (see Figure 8). Both membranes showed a similar behavior with regard to the hydrogen flow rate over 150 h. A small drop in the hydrogen permeation was detected after the long term test; for the $Pd_{95}Ag_5$ membrane from $5.71 \cdot 10^{-6}$ mol s^{-1} m^{-2} Pa^{-1} down to $4.15 \cdot 10^{-6}$ mol s^{-1} m^{-2} Pa^{-1} (27%) and also for the $Pd_{91.7}Ag_{4.8}Au_{3.5}$ membrane the hydrogen permeation decreased from $6.24 \cdot 10^{-6}$ to $4.77 \cdot 10^{-6}$ mol s^{-1} m^{-2} Pa^{-1} (24%). A similar decrease in the hydrogen permeance as a function of time at 600 °C has been observed by Abu El Hawa et al. [31] for a 4.9 μm thick Pd membrane during 250 h and for a 6.0 μm thick $PdRu_{0.3}$ membrane for almost 500 h. As described by Okazaki et al. [32], the hydrogen permeation flux through a 3.8 μm thick palladium membrane on an α-alumina support decreased markedly during the permeation tests conducted at temperatures above 600 °C due to the formation of a Pd-Al alloy (due to the

reduction of alumina to aluminum at high temperature in the presence of H_2 [32]). In this work, the zirconia layer on the outside of the support and in contact with the Pd alloy membrane, prevents the formation of any strong support interaction as reported by Okazaki et al. [32]. During the long-term test of the M1 and M1Au membranes the nitrogen permeation rate increased slowly leading to a decrease in the H_2/N_2 ideal perm-selectivity from 538 to 317 for $Pd_{94.9}Ag_{5.1}$ and from 378 to 244 for $Pd_{91.7}Ag_{4.8}Au_{3.5}$ membranes with a rate of $1.67 \cdot 10^{-11}$ and $2 \cdot 10^{-11}$ mol s^{-1} m^{-2} Pa^{-1} h^{-1} respectively at 600 °C for the 150 h test. According to the findings by Abu El Hawa et al. [31], the nitrogen leakages show higher rates (and their leakage flow rates were higher than those in this work) for a pure Pd membrane at the same operating temperature, whereas the addition of Pt or Ru to Pd films improved the thermal stability by lowering the rate at which the nitrogen leak flow grows in time at $3 \cdot 10^{-12}$ mol s^{-1} m^{-2} Pa^{-1} h^{-1}.
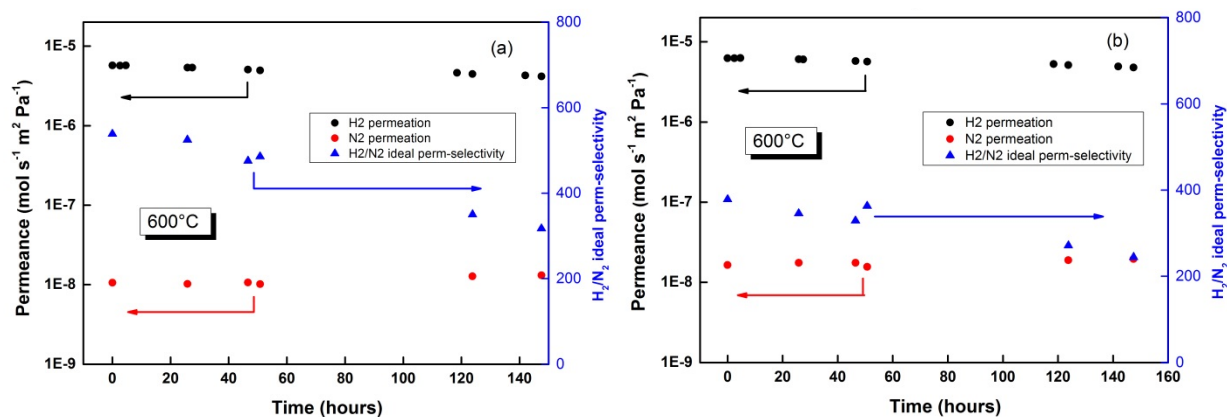

Figure 8. H_2 and N_2 permeances (mol m^{-2} s^{-1} Pa^{-1}) and H_2/N_2 ideal perm-selectivity of a) M1; and b) M1Au membranes for 150 h at 600 °C and 1 bar of pressure difference.

Three of the membranes prepared in this work, M2, M2Au and M3Au (see Table 1), were used to study their behavior under H_2S conditions at 550 °C. The effective length of the membranes after sealing was 14.67 mm, 30.65 mm and 11.16 mm respectively. Before being tested under atmospheres with a different H_2S content and for different times on stream, a comparison of the hydrogen fluxes of M2 ($Pd_{96.1}Ag_{3.9}$), M2Au ($Pd_{91.5}Ag_{4.7}Au_{3.8}$) and M3Au ($Pd_{90.5}Ag_{4.6}Au_{4.9}$) membranes was performed at 550 °C and transmembrane pressure differences up to 3 bar. The results of this characterization, prior to the H_2S exposure, are shown in Figure 9. Before testing the H_2 permeance, the membranes were activated following the same procedure used for the M1 and M1Au membranes. After the activation, the membranes were left in pure H_2 until a stable flux through the membrane was obtained. The obtained initial H_2 permeance for the

membranes M2 ($Pd_{96.1}Ag_{3.9}$), M2Au ($Pd_{91.5}Ag_{4.7}Au_{3.8}$) and M3Au ($Pd_{90.5}Ag_{4.6}Au_{4.9}$) are $1.7 \cdot 10^{-3}$, $2.3 \cdot 10^{-3}$ and $3.9 \cdot 10^{-3}$ mol s^{-1} m^{-2} $Pa^{-0.5}$ respectively. The calculated H_2/N_2 ideal perm-selectivity was above 1850 for all these membranes, since the measured N_2 leakage flow rate was below the detection limit of the flow meter (0.2 mL/min). As shown in the previous results at 550 °C, the Pd-Ag-Au membranes have higher permeances than the Pd-Ag membrane. The H_2 permeance obtained with the single gas tests is used as a reference for the H_2S exposure and recovery results.
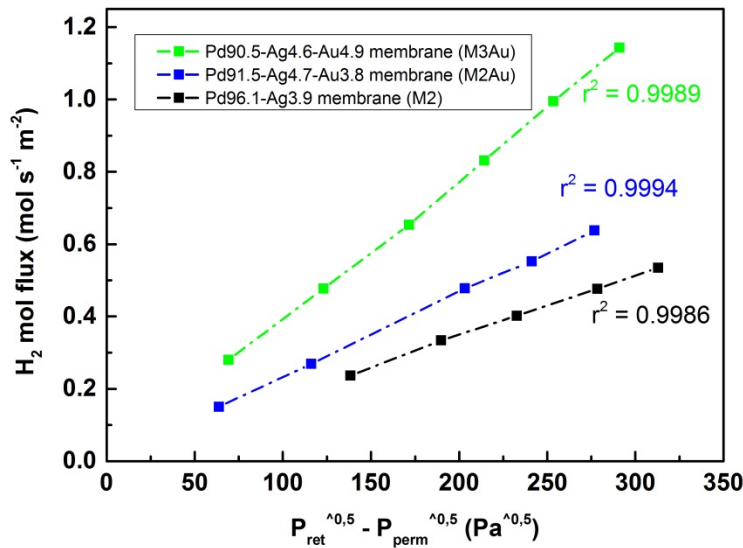

Figure 9. H_2 flux of membranes $Pd_{96.1}Ag_{3.9}$ (M2), $Pd_{91.5}Ag_{4.7}Au_{3.8}$ (M2Au) and M3 $Pd_{90.5}Ag_{4.6}Au_{4.9}$ (M3Au) as a function of H_2 difference of square root of the pressure at 550 °C

Table 2 compares the Pd-Ag-Au membranes prepared in this work with the permeation properties of some of the best membranes reported in the literature. The membranes prepared in this work showed the highest hydrogen permeance ever reported among those fabricated by ELP. Only those reported by Peters et al. (a $Pd_{75}Ag_{22}Au_3$ membrane of 1.9 μm thickness [18] and a $Pd_{95}Au_5$ membrane of 2.5 μm [33]) prepared by sputtering showed an even higher hydrogen permeance at 400 °C and 450 °C. There is not a clear trend regarding the comparison between a Pd or Pd-Ag membrane and another one alloyed with gold. The hydrogen permeance differs by almost a factor 2 when comparing the M1Au with M2Au membranes, despite the fact the membranes have a similar composition. The observed difference cannot be justified only by a difference in the thicknesses of the membranes, which is only 0.4 μm, and the observed discrepancy needs to be a consequence of other factors that have not yet been determined. A strict comparative analysis regarding the hydrogen recovery after H_2S exposure

of the different membranes tested in the literature is more difficult because of the large variety in H_2S concentrations and times of exposure studied in each work.

Table 2. Summary of the H_2 permeance of different Pd-based membranes alloyed with Au and their exposure conditions to H_2S reported in the literature and the ones presented in this work.

Membrane /support	Thickness (µm)	Preparation method	Temperature (°C)	H_2 permeance [(10^{-3} mol s^{-1} m^{-2} Pa$^{0.5}$)]	H_2 permeance over pure Pd (%) *	H_2S treatment / Recovery	Reference
Pd$_{75}$Ag$_{22}$Au$_3$ / micro-channel	1.9	Sputtering	400	4.47	82 (over Pd$_{77}$Ag$_{23}$)	-	[18]
Pd$_{75}$Ag$_{22}$Au$_3$ / micro-channel	1.9	Sputtering	450	4.89	83 (over Pd$_{77}$Ag$_{23}$)	20 ppm / 1 hour / 90% H2–N2. ~80% flux recovery	[18]
Pd$_{75}$Ag$_{16}$Au$_9$ / ZrO2-modified porous stainless steel (PSS) disk	~ 14	ELP	400	0.84	98	100 ppm / 24 hours. 65% flux recovery	[13]
Pd$_{75}$Ag$_{16}$Au$_9$ / ZrO2-PSS disk	~ 14	ELP	450	0.97	90	-	[13]
Pd$_{78}$Ag$_9$Au$_{13}$ / ZrO2-PSS disk	~ 14	ELP	400	0.96	111	100 ppm / 24 hours. 80% flux recovery	[13]
Pd$_{78}$Ag$_9$Au$_{13}$ / ZrO2-PSS disk	~ 14	ELP	450	1.16	107	-	[13]
Pd$_{95}$Au$_5$ / micro-channel	2.5	Sputtering	400	4.40	113	-	[33]
Pd$_{72}$Cu$_{25}$Au$_3$ / micro-channel	2.1	Sputtering	400	1.81	38	-	[33]
Pd$_{91}$Au$_9$-ZrO$_2$ / PSS disk	12	ELP	400	0.92	-	-	[34]
Pd$_{91}$Au$_9$-ZrO$_2$ / PSS disk	12	ELP	450	1.25	-	-	[34]
Pd$_{92}$Au$_8$ / PSS plates	18.1	ELP & Galvanic displacement plating	500	0,26	13	54.8 ppm / 4 hours. 65% flux recovery	[6]
PdAu$_{20}$	25	Cold worked	400	0.40	-	20 ppm / 100 hours in 51% H2; 29% CO2; 19% H2O; 1%	[17]

Membrane	*	Method	T (°C)			CO stream	Ref.
						CO stream	
Pd$_{83}$Ag$_2$Au$_{15}$ / ZrO$_2$-PSS disk	14.0	ELP	400	0,93	108	100 ppm / 24 hours. 32% flux recovery	[20]
PdAu$_{20}$Ag$_{13}$ / ZrO$_2$-PSS tubes	9.3	ELP	400	~ 0.95	-	20 ppm / 24 hours. 70% flux recovery	[19]
			450	~ 1.1	-	20 ppm / 24 hours. 93% flux recovery	[19]
			500	~ 1.45	-	20 ppm / 24 hours. 85-90% flux recovery	[19]
M1Au. Pd$_{91.7}$Ag$_{4.8}$Au$_{3.5}$ / ZrO$_2$ ceramic porous tubes	2.71	ELP	400	2.52	81 (over Pd$_{94.9}$Ag$_{5.1}$)	-	[this wok]
		ELP	450	3.21	91 (over Pd$_{94.9}$Ag$_{5.1}$)	-	[this wok]
		ELP	500	3.69	96 (over Pd$_{94.9}$Ag$_{5.1}$)	-	[this wok]
		ELP	550	4.27	102 (over Pd$_{94.9}$Ag$_{5.1}$)	-	[this wok]
		ELP	600	4.71	104 (over Pd$_{94.9}$Ag$_{5.1}$)	-	[this wok]
M2Au. Pd$_{91.5}$Ag$_{4.7}$Au$_{3.8}$ / ZrO$_2$ ceramic porous tubes	3.13	ELP	550	2.32	135 (over Pd$_{96.1}$Ag$_{3.9}$)	9 ppm / 12.5 hours. 85 % recovery	[this wok]
M3Au. Pd$_{90.5}$Ag$_{4.6}$Au$_{4.9}$ / ZrO$_2$ ceramic porous tubes	2.31	ELP	550	3.91	-	17 ppm / 12.5 hours. 83 % recovery	[this wok]

* H$_2$ permeance of each membrane over the Pd membrane developed in each study.

3.2.2 H_2S exposure tests

At the end of the pure hydrogen permeation experiments with M2 ($Pd_{96.1}Ag_{3.9}$), M2Au ($Pd_{91.5}Ag_{4.7}Au_{3.8}$) and M3Au ($Pd_{90.5}Ag_{4.6}Au_{4.9}$) membranes, a sequence of different H_2S contents (in ppm) were added to the hydrogen feed gas to investigate the effect of H_2S on the hydrogen permeation rate at 550 ºC and 1 bar of pressure difference. In Table 3, the concentration of H_2S and time of exposure to H_2S are shown. M2 ($Pd_{96.1}Ag_{3.9}$) was exposed for 15.25 h in total at 1 H_2S ppm (10 h and 15 min) and 3 H_2S ppm (5 h), whereas the $Pd_{91.5}Ag_{4.7}Au_{3.8}$ and $Pd_{90.5}Ag_{4.6}Au_{4.9}$ membranes were exposed for 2.5 h to H_2S at each concentration. The H_2 permeation rate was measured before and after each H_2S inhibition test and the determined relative H_2 permeance before and after exposure at the different H_2S concentrations is shown in Figure 10a. Subsequently, the feed gas was changed back to pure H_2 and the temperature was increased to 600 °C to desorb the sulfur that was reversibly bonded [6]. The recovery step was carried out for 1 h, which allowed reaching a stable H_2 permeance through the membranes. The relation between the H_2 permeance before the H_2S exposure and after recovery is shown in Figure 10b. Post-characterization based on XRD, XPS and SEM analysis was used to investigate the effect of the H_2S exposure on the membrane after all the tests were completed.

Table 3. Concentration of H_2S on exposure and total time of exposure for each membrane.

Membrane	1 ppm	3ppm	5ppm	7ppm	9ppm	13ppm	17ppm	Total time of exposure [h]	H2/N2 ideal perm-selectivity after H_2S tests
M2 ($Pd_{96.1}Ag_{3.9}$)	X	X			X*			15.25	18
M2Au ($Pd_{91.5}Ag_{4.7}Au_{3.8}$)	X	X	X	X	X			12.5	793
M3Au ($Pd_{90.5}Ag_{4.6}Au_{4.9}$)	X		X		X	X	X	12.5	121

* At 9 ppm, H_2 flux was entirely inhibited, so the permeation test under H_2S exposure was suspended.

For the M2 ($Pd_{96.1}Ag_{3.9}$) membrane exposed to 1 ppm of H_2S, a decrease of 38% in the H_2 permeation rate was observed, caused by the interaction of H_2S with active sites on the membrane surface blocking the H_2 dissociation sites [18], [35], [36], [37]. After the initial decrease, no further significant decrease in the flux was measured during the exposure. A permanent decrease in the flux during the exposure is expected when bulk sulfides are formed, which have a lower H_2 permeability than the Pd-Ag alloy membrane [4], [9]. The H_2 permeance

obtained after a 1 h of recovery under pure H_2 at 600 °C was only 52% of the initial permeance before the exposure to 1 ppm H_2S leading to an incomplete recovery from sulfur poisoning. This could be explained by the formation of irreversible bulk sulfides in some areas of the membrane. During the exposure to 3 ppm H_2S a reduction in the permeance of 39% of the initial permeance was observed. The recovery after the exposure of 3 ppm of H_2S resulted in 55% of the initial permeance. During the exposure of 9 ppm the flux decreased below detectable values for the permeate flow rate measurement, which indicates that a full poisoning of the Pd-Ag layer occurred and that there are not large defects in the membrane. However, the thermodynamic equilibrium for Pd_4S formation at 550 °C and 100% H_2 takes place at 28.5 ppm of H_2S as reported by Mundschau et al. [9]. After the recovery, the hydrogen flux was twice the initial flux with a H_2/N_2 ideal perm-selectivity of 18. The very large increase in the hydrogen permeance may suggest that some kind of corrosion has occurred during the hydrogen recovery step. As can be seen in Figure 11, when the M2 membrane (A) was removed from the setup, its surface had lost its initially shiny grey look and had turned into an "unpolished" appearance, whereas membranes the gold alloyed membranes (B and C) remained shiny.
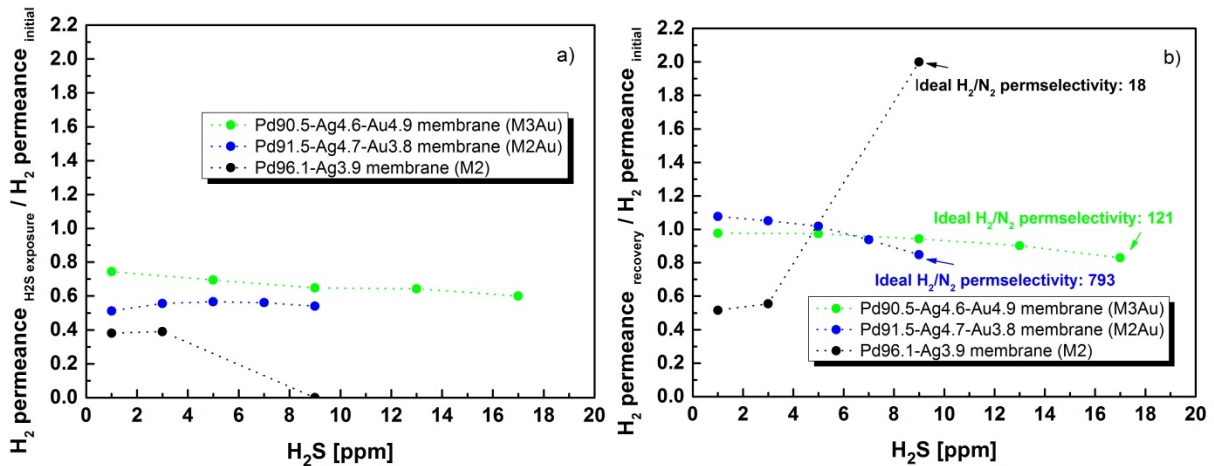

Figure 10. a) H_2 permeance normalized with initial permeance during exposure for different concentrations of H_2S at 550 °C, and b) H_2 permeance after recovery normalized with initial permeance after recovery for different concentrations of H_2S at 550 °C.
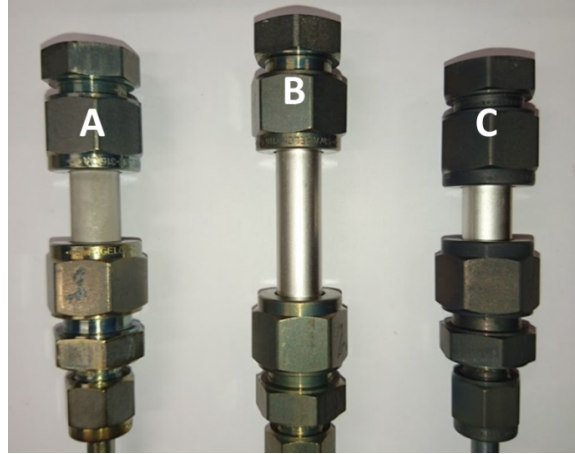
Figure 11. $Pd_{96.1}Ag_{3.9}$ (A), $Pd_{91.5}Ag_{4.7}Au_{3.8}$ (B), and $Pd_{90.5}Ag_{4.6}Au_{4.9}$ (C) membranes after testing under H_2S conditions.

The M2Au was first exposed to 1 ppm of H_2S, resulting in 51% of the initial permeance. The lower decrease in the flux compared to the M2 membrane was expected due to the presence of gold. According to Hyman et al. [38] the lower poisoning effect by Au addition is due to the higher energy barrier for H_2S to dissociate on gold. This was also demonstrated by Peters et al. [18] for ternary Pd membranes with gold [18]. After the recovery, the permeance obtained is even higher than the initial, exactly 107%. The following tests under 3, 5, 7 and 9 ppm H_2S showed a slight increase after each exposure. The increasing trend was, however, not observed after the recovery, so that hydrogen permeance ends at 85% of its initial flux after the 9 ppm test. The M3Au membrane exhibited an almost similar behavior as the M2Au membrane, regarding its hydrogen permeance after recovery, but with a lower poisoning effect under H_2S exposure, probably due to its higher Au content. For both M2Au and M3Au membranes, the decrease after recovery can be explained by either irreversibly adsorbed sulfur or the formation of bulk sulfides. The effect of irreversibly adsorbed sulfur or bulk sulfides is more pronounced for exposures at higher H_2S concentrations, which leads to the decrease in permeance.

Although the extent of recovery after the H_2S exposition is almost similar for the M3Au and M2Au membranes, the decrease in the H_2 permeance during the H_2S exposure under the same conditions is lower for the M3Au membrane, probably due to its higher Au content. The selectivity was only determined after the last exposure and was not measured during the experiment. As mentioned before, the M2 membrane ($Pd_{96.1}Ag_{3.9}$) had a perm-selectivity of 18 after exposure to 9 ppm H_2S for 15.25 h. The selectivity obtained for the M2Au ($Pd_{91.5}Ag_{4.7}Au_{3.8}$) and M3Au ($Pd_{90.5}Ag_{4.6}Au_{4.9}$) membranes are respectively 793 after 9 ppm and 12.5 h and 121

after 17 ppm and 12.5 h. The results show that the decrease in selectivity is less pronounced when gold is present in the membrane.

3.2.3 Characterization of the membranes after the H₂S test

Post characterization based on XRD, XPS and SEM analysis was carried out to investigate the effect of sulfur on the H_2 permeance once all the permeation tests were finalized. The outer surfaces of the membranes were analyzed using SEM (Figure 12). Figures 12a, 12c and 12e are the SEM images of membrane surfaces after the annealing treatment (but before any permeation test), whereas Figures 12b, 12d and 12f show the corresponding results after the H_2/H_2S testing. The SEM micrographs of the M2Au sample (Figure 12c) show that the Au cluster structure of the surface has already merged with the previous Pd-Ag structure. After the H_2/H_2S tests, the Pd-Ag-Au samples in Figure 12f show that full fusion of Au particles with the underlying layer has taken place as a result of the long-term testing at 550 ºC and subsequent alloying has occurred. The complete alloying of both Pd-Ag-Au layers was also verified by XRD, shown in Figure 14. The appearance of the Pd-Ag-Au membrane surface after testing is similar to the one reported by [3] for Pd-Au layers after 96 h at 550 ºC.

After the H_2S tests, for all the samples, the formation of polyhedral structures is observed which is more pronounced for the Pd-Ag membrane when Au is not present (Figure 12b), where spaces are formed between the structures indicating loss of material. An increase in the gold content decreases the tendency to form these structures (see Figure 12d and Figure 12f). The formation of these structures was also reported by Peters et al. [39] for a PdAg₄ sample indicating that surface roughening and grain growth also occurred during H_2S exposure to 20 ppm for 265 h at 450 ºC. A high sulfur concentration was observed (15 at% according to EDS analysis) confirming severe sulfide formation. Similar results were obtained by Braun et al. [20] where a Pd foil revealed the appearance of discrete surface aggregates after 3 h under 1000 ppm H_2S exposure at 400 ºC. These aggregates grew until they covered the entire surface after 30 h under the same conditions and X-ray characterization confirmed the presence of S in the aggregates of this Pd foil. Nevertheless, no sulfur compounds were detected for the M2 membrane by characterization techniques such as EDS, XRD and XPS. The absence of sulfur compounds completely covering the surface can be attributed to the recovery step, where hydrogen removed the absorbed sulfur, thereby damaging the Pd-Ag layer and leading to a

corrosion effect. The cross-section of the M1 membrane in Figure 13 shows that material was lost and that the membrane became thinner after H_2S exposure (Figure 13b), which could be responsible of the significant increase in the hydrogen flux, which was almost double after sulfur tests (Figure 10b). Braun et al. [13] reported defect formation for different Pd-Ag-Au alloys and after 24 h under 100 ppm H_2S exposure at 400 ºC. Moreover, Gade et al. [17] analyzed two Pd-Au membranes ($PdAu_{7.0}$ and $PdAu_{10.1}$) fabricated by sputtering, and they observed a reduction of their thicknesses from 11 μm to 3.3 μm and from 31 μm to 26 μm respectively after water-gas-shift (WGS) tests at 400 °C with 20 ppm of H_2S.
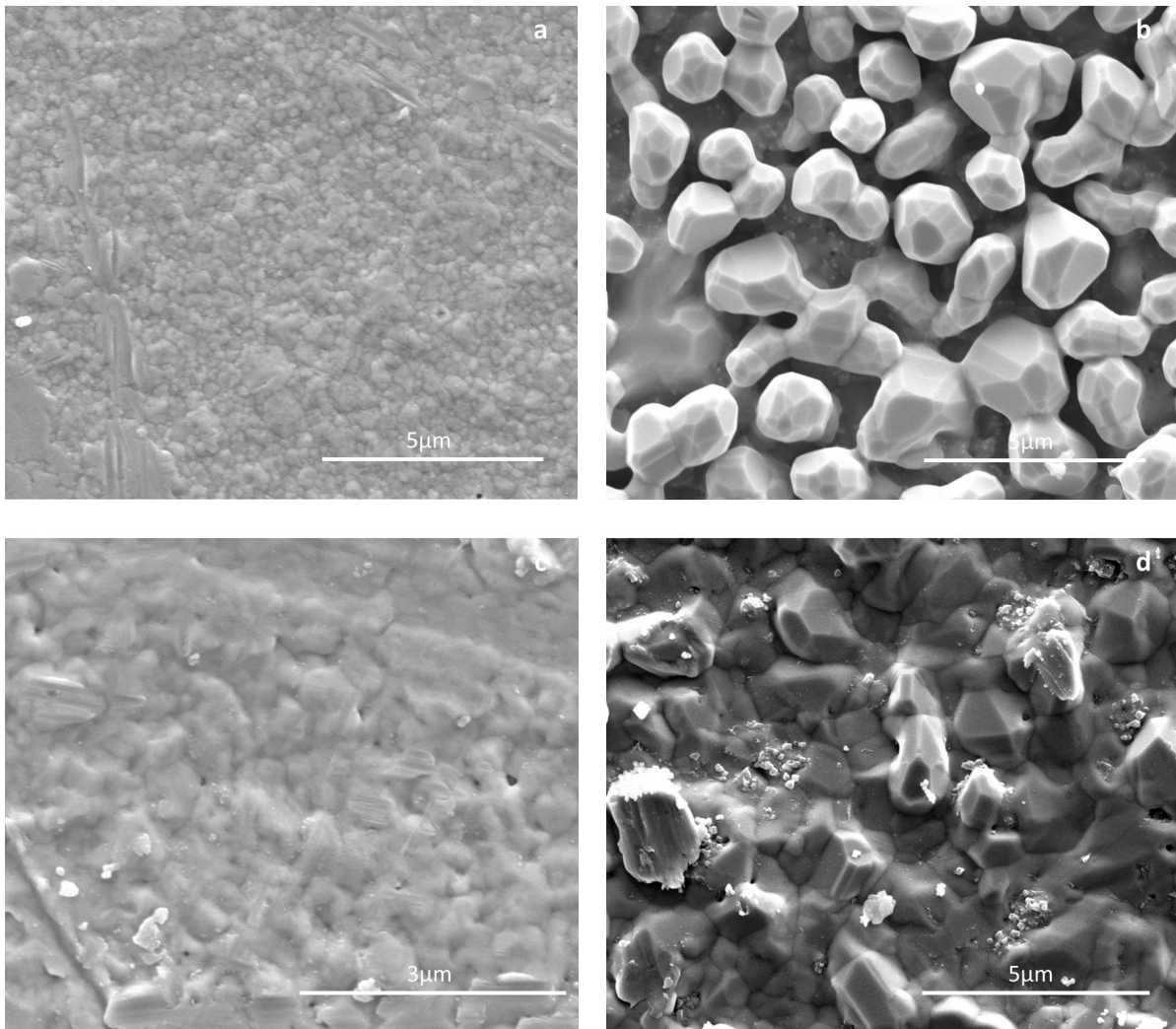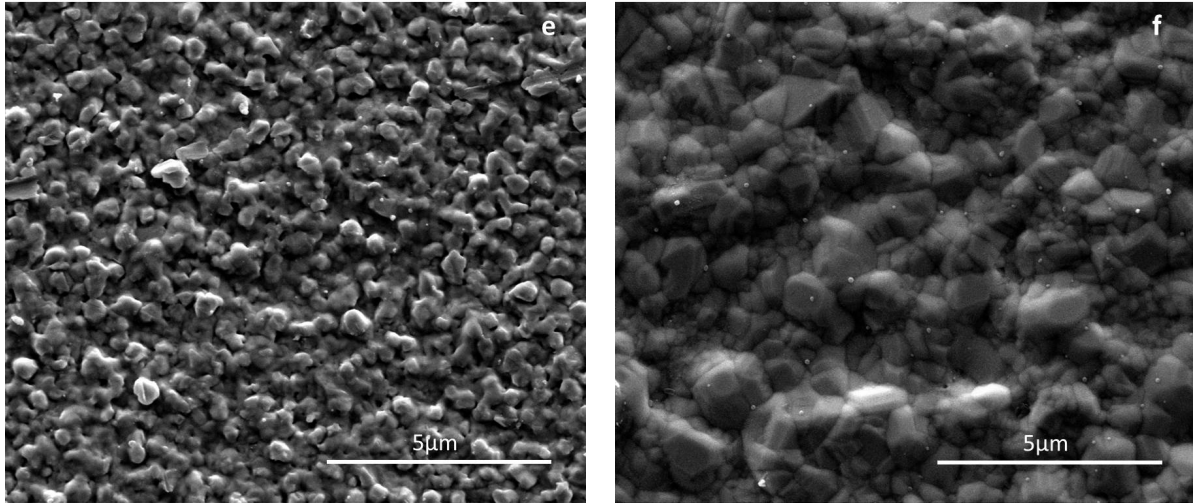
Figure 12. SEM surface images of a) $Pd_{96.1}Ag_{3.9}$ (M2) before testing; b) $Pd_{96.1}Ag_{3.9}$ (M2) after testing under H_2S conditions; c) $Pd_{91.5}Ag_{4.7}Au_{3.8}$ (M2Au) before testing; d) $Pd_{91.5}Ag_{4.7}Au_{3.8}$ (M2Au) after testing under H_2S conditions; e) $Pd_{90.5}Ag_{4.6}Au_{4.9}$ (M3Au) before testing; f) $Pd_{90.5}Ag_{4.6}Au_{4.9}$ (M3Au) after testing under H_2S conditions.

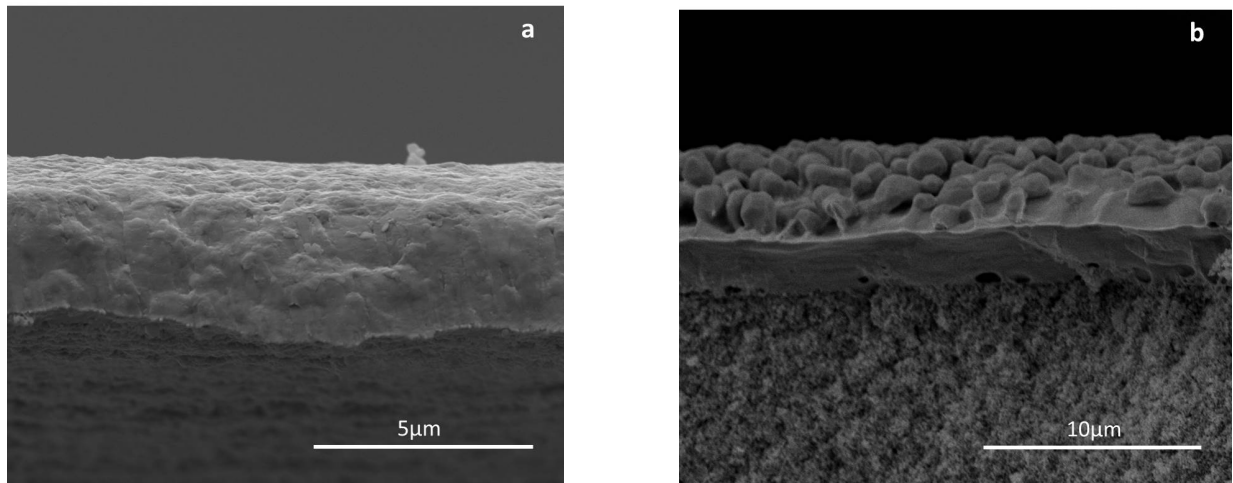**Figure 13.** SEM cross-section images of a) M2 ($Pd_{96.1}Ag_{3.9}$) prior to permeation tests and b) M2 ($Pd_{96.1}Ag_{3.9}$) after testing under H_2S conditions

In order to determine whether bulk sulfides were formed on the membrane surface during the tests, the metal films were removed from the ceramic support before the XRD analysis. Figure 14 shows the X-ray diffraction patterns obtained for the $Pd_{96.1}Ag_{3.9}$ and $Pd_{91.5}Ag_{4.7}Au_{3.8}$ membranes before and after H_2 exposure tests. The M2 ($Pd_{96.1}Ag_{3.9}$) peaks are symmetric indicating that complete annealing was achieved before any H_2S test. After H_2S exposure, these

diffracted peaks suffered a small deformation, indicating the start of dealloying, as reported by Lewis et al. [19] for $PdAu_{23}$ and $PdAu_{20}Ag_{13}$ membranes after 24 h exposure of 20 ppm of H_2S in H_2 as feed gas and subsequent tests under WGS feed conditions. However, there are no signs of clear sulfide peaks. As was reported for the M2($Pd_{96.1}Ag_{3.9}$) membrane after H_2S exposure, only a starting depletion of the Pd-Ag main diffraction peaks is described by Lewis et al. [19] due to the sulfide effect, compared to the Pd-Ag peak before any permeation tests. Regarding the M2Au ($Pd_{91.5}Ag_{4.7}Au_{3.8}$) membrane, the peaks before testing are not symmetric, which indicates that alloying was not yet complete. The M2Au ($Pd_{91.5}Ag_{4.7}Au_{3.8}$) membrane after the 12.5 h test under H_2S exposure shows sharp diffracted peaks, from which it is concluded that after all the tests complete annealing was reached. Moreover, no sulfur and bulk sulfide phases were detected.
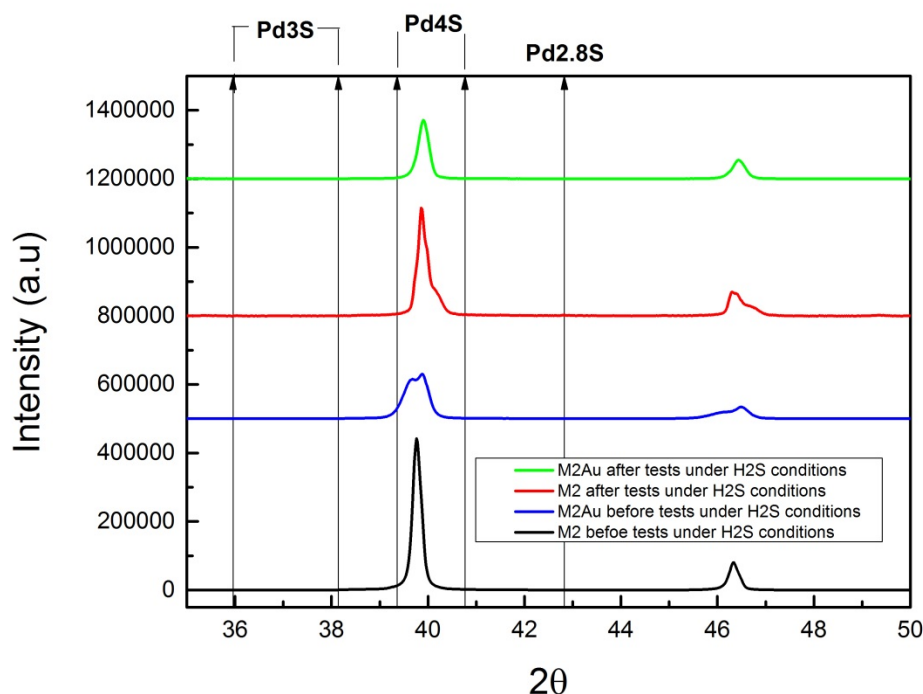

Figure 14. X-ray diffraction patterns of M2 and M2Au membranes before and after H_2S exposure. H_2S treatment conditions listed in Table 3.

Figure 15a–e shows the XPS depth profiles, where the atomic compositions as a function of the XPS etching time is obtained for Pd-Ag based membranes exposed to different H_2S concentrations. The XPS analysis is performed on the membrane prior to exposure and after the H_2S tests. The composition of the $Pd_{96.1}Ag_{3.9}$ membrane did not change significantly after its exposure to H_2S. The amount of sulfur found on the surface in the beginning of the

characterization were 1.71 at% in M2, 2.8 at% in M2Au and 8.7 at% in M3Au but these values were rapidly reduced to almost 0 at% in all the samples indicating that there was not any remaining sulfur. These values are very small compared to those found by Peters et al. [18], but the total time of exposure was much longer in that study. The undetectably low hydrogen permeation rate found for the Pd-Ag membrane under 9 ppm of H_2S (Figure 11a), but lack of sulfur presence throughout the XPS test, suggests that the recovery step carried out under a H_2 stream at 600 ºC during 1 h removed the Pd-S structure. The remainder of sulfur detected is expected to be either bulk sulfides or irreversible adsorbed sulfur [40].

Regarding the M2Au and M3Au membranes, in both samples the palladium content increases on the surface compared to their values prior to exposure. The migration of Pd to the surface of the membrane after testing could be explained by the lack of total annealing (in terms of time and/or temperature). It also explains the increase in the permeance found for $Pd_{91.5}Ag_{4.7}Au_{3.8}$, since it needed a longer activation time to reach a stable permeance prior to exposure. The gold content on the surface of the M3Au is higher than in the M2Au membrane, as expected due to the higher Au amount added in the ELP deposition process. For both gold containing samples, with an increase in the etching time, there is a slight decrease in the palladium concentration and an increase in the gold concentration, while the silver concentration remained constant.

In other studies, the increase in the Pd content on the feed-side surface after H_2S exposure, corroborates Au surface depletion on the feed side after H_2S testing reported by Lewis et al. [19] for two Pd-Ag-Au membranes fabricated by ELP. Gade et al. [17] also described lower contents of Au on their surfaces after testing. However, these values are still higher than the ones calculated as the theoretical ones added during the Au electroless plating. This observation can be explained by incomplete annealing or by Au surface segregation, as reported by Gade et al. [26] for Pd-Au membranes prepared by sequential electroless plating, where an unalloyed layer of pure Pd remained below the gold. In addition, Au was the last metal to be deposited during the electroless plating process. It is possible that due to a too low annealing temperature and/or too short annealing time, complete homogenization may not have been accomplished throughout this process, and this would explain why the surface was Au enriched [19].
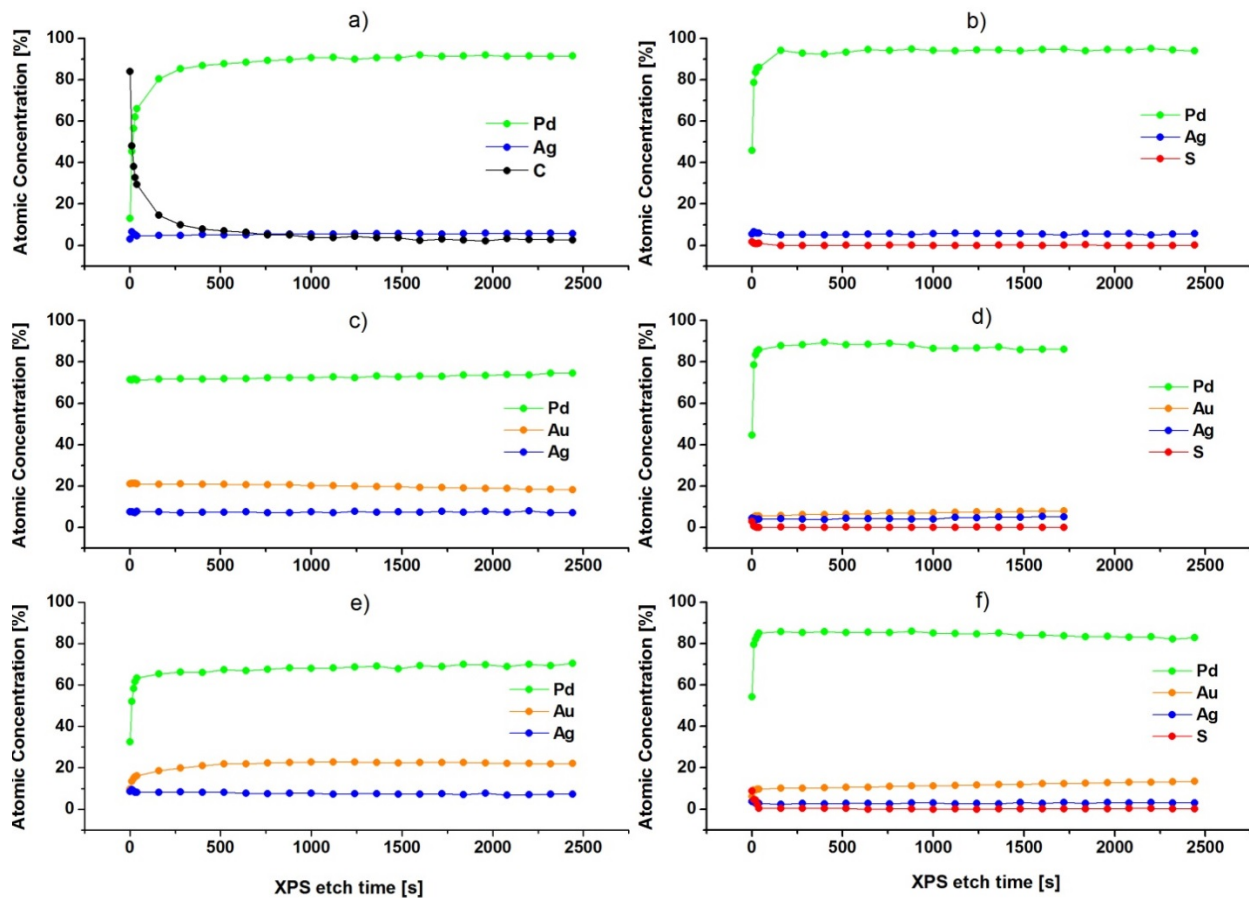
Figure 15. XPS depth profiles; a) M2 ($Pd_{96.1}Ag_{3.9}$) prior to exposure; b) M2 ($Pd_{96.1}Ag_{3.9}$) after exposure; c) M2Au ($Pd_{91.5}Ag_{4.7}Au_{3.8}$) prior to exposure, d) M2Au ($Pd_{91.5}Ag_{4.7}Au_{3.8}$) after exposure; e) M3Au ($Pd_{90.5}Ag_{4.6}Au_{4.9}$) prior to exposure and f) M3Au ($Pd_{90.5}Ag_{4.6}Au_{4.9}$) after exposure.

4. Conclusions

Pd-Ag-Au membranes were prepared by Au deposition by electroless plating on PdAg membranes. In order to study the effect of the addition of Au, half of the membrane was plated with Au leaving the other half with only PdAg. Hydrogen permeation properties were studied providing a fair comparison of the effect of gold. The $Pd_{91.7}Ag_{4.8}Au_{3.5}$ membrane showed a higher hydrogen permeation rate than the $Pd_{94.9}Ag_{5.1}$ membrane above 550 ºC. The Pd-Ag and Pd-Ag-Au membranes exhibited a slight decrease in their hydrogen flux and a small increase in the nitrogen fluxes over the 150 h test at 600 ºC. A H_2 permeance of $4.71 \cdot 10^{-3}$ mol s^{-1} m^{-2} Pa$^{0.5}$ at 600 °C was obtained for the $Pd_{91.7}Ag_{4.8}Au_{3.5}$ membrane that had a thickness of 2.71 µm. The activation energy for the H_2 flux through the $Pd_{94.9}Ag_{5.1}$ membrane was determined at

9.5 kJ·mol^{-1}. However, after the addition of Au, the activation energy was found to increase up to 16.0 kJ·mole^{-1}, showing that the addition of Au has an effect on the adsorption and dissociation steps in the solution-diffusion model of the H$_2$ transport through Pd-based membranes. This was also corroborated with the regression factor values obtained for different values for *n* in Sieverts' equation, where *n* is very close to 0.5 for Pd-Ag and increases to 0.7-0.8 after the addition of Au. The H$_2$ permeance of Pd-Ag and Pd-Ag-Au membranes with different gold compositions was measured under exposure to H$_2$S for different H2S concentrations and exposure times and after recovery. The addition of Au to the Pd-Ag membranes increases the resistance to H$_2$S poisoning. The H$_2$/N$_2$ ideal perm-selectivity of Pd-Ag-Au membranes was maintained better after H$_2$S exposure compared to the Pd-Ag membranes. However, the decrease in the selectivity after exposure is still substantial. The membranes exposed to H$_2$S, showed that sulfur has an effect on the surface of the membranes by the formation of polyhedral crystals after testing and removing H$_2$S. The formation these of polyhedral structures produce corrosion in the Pd-Ag membrane, increasing the hydrogen permeation. This phenomenon is less pronounced when Au is added.

Acknowledgements

References

[1] B.G.S. Burkhanov, N.B. Gorina, N.B. Kolchugina, N.R. Roshan, D.I. Slovetsky, E.M. Chistov, Palladium-Based Alloy Membranes for Separation of High Purity Hydrogen from Hydrogen-Containing Gas Mixtures, Platin. Met. Rev. 55 (2011) 3–12. doi:10.1595/147106711X540346.

[2] O. Veneri, Hydrogen as Future Energy Carrier, in: Hydrog. Fuel Cells Road Veh., Springer Berlin Heidelberg, 2011: pp. 33–70. doi:10.1007/978-0-85729-136-3_2.

[3] C. Chao-Huang, Sulfur tolerance of Pd/Au alloy membranes for hydrogen separation from coal gas, Worcester Polytechnic Institute, 2011.

[4] C.P. O'Brien, A.J. Gellman, B.D. Morreale, J.B. Miller, The hydrogen permeability of Pd4S, J. Memb. Sci. 371 (2011) 263–267. doi:10.1016/j.memsci.2011.01.044.

[5] B.D. Morreale, Bret H. Howard, O. Iyoha, R.M. Enick, A. Chen Ling, D.S. Sholl§, Experimental and Computational Prediction of the Hydrogen Transport Properties of Pd4S, (2007). doi:10.1021/IE070461U.

[6] C.-H. Chen, Y.H. Ma, The effect of H2S on the performance of Pd and Pd/Au composite membrane, J. Memb. Sci. 362 (2010) 535–544. doi:10.1016/j.memsci.2010.07.002.

[7] A. Basile, A. Iulianelli, T. Longo, S. Liguori, M. De Falco, Pd-based Selective Membrane State-of-the-Art, in: Membr. React. Hydrog. Prod. Process., Springer London, London, 2011: pp. 21–55. doi:10.1007/978-0-85729-151-6_2.

[8] D.L. Mckinley, Metal alloy for hydrogen separation and purification, US3350845 A, 1965.

[9] M.V. Mundschau, X. Xie, C.R. Evenson, A.F. Sammells, Dense inorganic membranes for production of hydrogen from methane and coal with carbon dioxide sequestration, Catal. Today. 118 (2006) 12–23. doi:10.1016/j.cattod.2006.01.042.

[10] A. Kulprathipanja, G.O. Alptekin, J.L. Falconer, J.D. Way, Pd and Pd–Cu membranes: inhibition of H2 permeation by H2S, J. Memb. Sci. 254 (2005) 49–62. doi:10.1016/j.memsci.2004.11.031.

[11] J.B. Miller, B.D. Morreale, A.J. Gellman, The effect of adsorbed sulfur on surface segregation in a polycrystalline Pd70Cu30 alloy, Surf. Sci. 602 (2008) 1819–1825. doi:10.1016/j.susc.2008.03.018.

[12] N.A. Al-Mufachi, N.V. Rees, R. Steinberger-Wilkens, Hydrogen selective membranes: A review of palladium-based dense metal membranes, Renew. Sustain. Energy Rev. 47 (2015) 540–551. doi:10.1016/j.rser.2015.03.026.

[13] F. Braun, A.M. Tarditi, J.B. Miller, L.M. Cornaglia, Pd-based binary and ternary alloy membranes: Morphological and perm-selective characterization in the presence of H2S, J. Memb. Sci. 450 (2014) 299–307. doi:10.1016/j.memsci.2013.09.026.

[14] B.. Morreale, M.. Ciocco, B.. Howard, R.. Killmeyer, A.. Cugini, R.. Enick, Effect of hydrogen-sulfide on the hydrogen permeance of palladium–copper alloys at elevated temperatures, J. Memb. Sci. 241 (2004) 219–224. doi:10.1016/j.memsci.2004.04.033.

[15] E. Acha, J. Requies, V.L. Barrio, J.F. Cambra, M.B. Güemez, P.L. Arias, Y.C. van Delft,

PdCu membrane applied to hydrogen production from methane, J. Memb. Sci. 415 (2012) 66–74. doi:10.1016/j.memsci.2012.04.038.

[16] S. Yun, S. Ted Oyama, Correlations in palladium membranes for hydrogen separation: A review, J. Memb. Sci. 375 (2011) 28–45. doi:10.1016/j.memsci.2011.03.057.

[17] S.K. Gade, S.J. DeVoss, K.E. Coulter, S.N. Paglieri, G.O. Alptekin, J.D. Way, Palladium–gold membranes in mixed gas streams with hydrogen sulfide: Effect of alloy content and fabrication technique, J. Memb. Sci. 378 (2011) 35–41. doi:10.1016/j.memsci.2010.11.044.

[18] T.A. Peters, T. Kaleta, M. Stange, R. Bredesen, Development of ternary Pd–Ag–TM alloy membranes with improved sulphur tolerance, J. Memb. Sci. 429 (2013) 448–458. doi:10.1016/j.memsci.2012.11.062.

[19] A.E. Lewis, H. Zhao, H. Syed, C.A. Wolden, J.D. Way, PdAu and PdAuAg composite membranes for hydrogen separation from synthetic water-gas shift streams containing hydrogen sulfide, J. Memb. Sci. 465 (2014) 167–176. doi:10.1016/j.memsci.2014.04.022.

[20] F. Braun, J.B. Miller, A.J. Gellman, A.M. Tarditi, B. Fleutot, P. Kondratyuk, L.M. Cornaglia, PdAgAu alloy with high resistance to corrosion by H2S, Int. J. Hydrogen Energy. 37 (2012) 18547–18555. doi:10.1016/j.ijhydene.2012.09.040.

[21] D.A. Pacheco Tanaka, M.A. Llosa Tanco, S. Niwa, Y. Wakui, F. Mizukami, T. Namba, T.M. Suzuki, Preparation of palladium and silver alloy membrane on a porous α-alumina tube via simultaneous electroless plating, J. Memb. Sci. 247 (2005) 21–27. doi:10.1016/j.memsci.2004.06.002.

[22] E. Fernandez, A. Helmi, K. Coenen, J. Melendez, J.L. Viviente, D.A. Pacheco Tanaka, M. van Sint Annaland, F. Gallucci, Development of thin Pd–Ag supported membranes for fluidized bed membrane reactors including WGS related gases, Int. J. Hydrogen Energy. 40 (2015) 3506–3519. doi:10.1016/j.ijhydene.2014.08.074.

[23] A. Helmi, E. Fernandez, J. Melendez, D. Pacheco Tanaka, F. Gallucci, M. van Sint Annaland, Fluidized Bed Membrane Reactors for Ultra Pure H2 Production—A Step forward towards Commercialization, Molecules. 21 (2016) 376. doi:10.3390/molecules21030376.

[24] J. Okazaki, D.A.P. Tanaka, M.A.L. Tanco, Y. Wakui, T. Ikeda, F. Mizukami, T.M. Suzuki, Preparation and Hydrogen Permeation Properties of Thin Pd-Au Alloy Membranes Supported on Porous α-Alumina Tube, Mater. Trans. 49 (2008) 449–452. doi:10.2320/matertrans.MBW200720.

[25] W. Chen, X. Hu, R. Wang, Y. Huang, On the assembling of Pd/ceramic composite membranes for hydrogen separation, Sep. Purif. Technol. 72 (2010) 92–97. doi:10.1016/j.seppur.2010.01.010.

[26] S.K. Gade, E.A. Payzant, H.J. Park, P.M. Thoen, J.D. Way, The effects of fabrication and annealing on the structure and hydrogen permeation of Pd-Au binary alloy membranes, J. Memb. Sci. 340 (2009) 227–233. doi:10.1016/j.memsci.2009.05.034.

[27] A. Iulianelli, M. Alavi, G. Bagnato, S. Liguori, J. Wilcox, M.R. Rahimpour, R. Eslamlouyan, B. Anzelmo, A. Basile, Supported Pd-Au Membrane Reactor for Hydrogen Production: Membrane Preparation, Characterization and Testing., Molecules. 21 (2016). doi:10.3390/molecules21050581.

[28] E. Fernandez, K. Coenen, A. Helmi, J. Melendez, J. Zuñiga, D.A. Pacheco Tanaka, M. Van Sint Annaland, F. Gallucci, Preparation and characterization of thin-film Pd-Ag supported membranes for high-temperature applications, Int. J. Hydrogen Energy. 40 (2015). doi:10.1016/j.ijhydene.2015.08.050.

[29] J. Catalano, M. Giacinti Baschetti, G.C. Sarti, Hydrogen permeation in palladium-based membranes in the presence of carbon monoxide, J. Memb. Sci. 362 (2010) 221–233. doi:10.1016/j.memsci.2010.06.055.

[30] V. Gryaznov, Metal containing membranes for the production of ultrapure hydrogen and the recovery of hydrogen isotopes, Sep. Purif. Rev. 29 (2000) 171–187. doi:10.1081/SPM-100100008.

[31] H.W. Abu El Hawa, S.N. Paglieri, C.C. Morris, A. Harale, J. Douglas Way, Identification of thermally stable Pd-alloy composite membranes for high temperature applications, J. Memb. Sci. 466 (2014) 151–160. doi:10.1016/j.memsci.2014.04.029.

[32] J. Okazaki, T. Ikeda, D.A. Pacheco Tanaka, M.A. Llosa Tanco, Y. Wakui, K. Sato, F. Mizukami, T.M. Suzuki, Importance of the support material in thin palladium composite membranes for steady hydrogen permeation at elevated temperatures., Phys. Chem. Chem. Phys. 11 (2009) 8632–8. doi:10.1039/b909401f.

[33] T.A. Peters, T. Kaleta, M. Stange, R. Bredesen, Development of thin binary and ternary Pd-based alloy membranes for use in hydrogen production, J. Memb. Sci. 383 (2011) 124–134. doi:10.1016/j.memsci.2011.08.050.

[34] A. Tarditi, C. Gerboni, L. Cornaglia, PdAu membranes supported on top of vacuum-assisted ZrO2-modified porous stainless steel substrates, J. Memb. Sci. 428 (2013) 1–10. doi:10.1016/j.memsci.2012.10.029.

[35] D.R. Alfonso, First-principles study of sulfur overlayers on Pd(111) surface, Surf. Sci. 596 (2005) 229–241. doi:10.1016/j.susc.2005.09.021.

[36] C.P. O'Brien, B.H. Howard, J.B. Miller, B.D. Morreale, A.J. Gellman, Inhibition of hydrogen transport through Pd and Pd47Cu53 membranes by H2S at 350°C, J. Memb. Sci. 349 (2010) 380–384. doi:10.1016/j.memsci.2009.11.070.

[37] C.P. O'Brien, J.B. Miller, B.D. Morreale, A.J. Gellman, H2/D2 Exchange Kinetics in the Presence of H2S over Pd4S, Pd70Cu30, and Pd47Cu53 surfaces, J. Phys. Chem. C. 116 (2012) 17657–17667. doi:10.1021/jp305024b.

[38] M.P. Hyman, B.T. Loveless, J.W. Medlin, A density functional theory study of H2S decomposition on the (111) surfaces of model Pd-alloys, Surf. Sci. 601 (2007) 5382–5393. doi:10.1016/j.susc.2007.08.030.

[39] T.A. Peters, M. Stange, P. Veenstra, A. Nijmeijer, R. Bredesen, The performance of Pd–Ag alloy membrane films under exposure to trace amounts of H2S, J. Memb. Sci. 499 (2016) 105–115. doi:10.1016/j.memsci.2015.10.031.

[40] N. Pomerantz, Y.H. Ma, Effect of H_2S on the Performance and Long-Term Stability of Pd/Cu Membranes, Ind. Eng. Chem. Res. 48 (2009) 4030–4039. doi:10.1021/ie801947a.